

## 3D Printing with Bamboo

### An Early-Stage Exploration Towards Its Use in the Built Environment

Wong, Jasmine; Aut, Serdar; Brancart, Stijn

**DOI**

[10.3390/su16114619](https://doi.org/10.3390/su16114619)

**Publication date**

2024

**Document Version**

Final published version

**Published in**

Sustainability

**Citation (APA)**

Wong, J., Aut, S., & Brancart, S. (2024). 3D Printing with Bamboo: An Early-Stage Exploration Towards Its Use in the Built Environment. *Sustainability*, 16(11), Article 4619. <https://doi.org/10.3390/su16114619>

**Important note**

To cite this publication, please use the final published version (if applicable).  
Please check the document version above.

**Copyright**

Other than for strictly personal use, it is not permitted to download, forward or distribute the text or part of it, without the consent of the author(s) and/or copyright holder(s), unless the work is under an open content license such as Creative Commons.

**Takedown policy**

Please contact us and provide details if you believe this document breaches copyrights.  
We will remove access to the work immediately and investigate your claim.

Article

# 3D Printing with Bamboo: An Early-Stage Exploration Towards Its Use in the Built Environment

Jasmine Wong, Serdar Aşut \* and Stijn Brancart

Department of Architectural Engineering and Technology, Faculty of Architecture and the Built Environment, Delft University of Technology, 2628 BL Delft, The Netherlands; jasmnewong2499@gmail.com (J.W.); s.brancart@tudelft.nl (S.B.)

\* Correspondence: s.asut@tudelft.nl

**Abstract:** Along with the circular bioeconomy principles, alternative ways of utilizing biomass waste streams are considered viable approaches to reaching sustainability goals. Accordingly, a growing body of literature is exploring new materials utilizing biomass in 3D-printing applications. This article presents early-stage research that initially investigates the usability of bamboo fibers and dust with bio-based binders in 3D printing towards its use in the design and production of the built environments. The research delves into solutions through a material tinkering approach to develop a bio-based composite material that can be used in fused deposition modeling (FDM). It includes mechanical strength analyses of printed specimens to understand the effects of different infill designs on the structural performance of objects printed using bamboo-based composite. Then, it demonstrates a design-to-production workflow that integrates a mechanically informed infill pattern within a self-supporting wall design that can be produced by 3D printing with bamboo. The workflow is presented with a partial demonstrator produced through robotic 3D printing. The article concludes with discussions and recommendations for further research.

**Keywords:** additive manufacturing; 3D printing; bio-based materials; bamboo; computational design; robotic fabrication; digital construction

**Citation:** Wong, J.; Aşut, S.; Brancart, S. 3D Printing with Bamboo: An Early-Stage Exploration Towards Its Use in the Built Environment. *Sustainability* **2024**, *16*, 4619. <https://doi.org/10.3390/su16114619>

Academic Editors: Szymon Skibicki, Marcin Hoffmann and Adam Zielinski

Received: 24 February 2024

Revised: 16 May 2024

Accepted: 17 May 2024

Published: 29 May 2024



**Copyright:** © 2024 by the authors. Licensee MDPI, Basel, Switzerland. This article is an open access article distributed under the terms and conditions of the Creative Commons Attribution (CC BY) license (<https://creativecommons.org/licenses/by/4.0/>).

## 1. Introduction

Rapid population growth is contributing to a considerable increase in the amount of raw materials used and produced worldwide [1]. The aim to create more ecologically friendly and sustainable construction processes has boosted interest in using bio-based materials. Bamboo, a non-wood species, holds promise as a potential sustainable construction material due to its rapid growth rate, being renewable, and being an adaptable plant that can grow well in a variety of climates and elevations [2].

This research aims to redefine the utilization of bamboo in construction. In many cases, the production of bamboo-based products generates waste material or by-products, which are frequently discarded, leading to unnecessary material wastage. To address this environmental concern and promote sustainability, we propose a method that harnesses bamboo as powder and fibers to create innovative new products. This approach aligns with the principles of the circular bioeconomy, offering a solution to mitigate material wastage and contribute to environmental conservation efforts. Within the circular bioeconomy, biomass is projected to play a key role in meeting global climate targets and moving towards a more circular bioeconomy by increasingly considering wastes and residues as a resource, investigating options for integrated biorefineries, and putting more focus on material and high-value applications of biomass [3]. A promising technology that can facilitate the utilization of bamboo powder and fibers in this manner is additive manufacturing (AM), also called 3D printing. AM techniques have seen significant advancements in the last few decades and have also made their way into the building sector. These

technologies offer the potential to reduce labor costs, minimize material waste, and enable the fabrication of complex geometries that are challenging to achieve using conventional production methods. While AM technologies have made significant progress for materials like plastics, concrete, clay, and steel, research on and application of AM using bamboo for architectural purposes is missing.

This research addresses this gap by exploring bamboo's usability in AM applications and developing a design and manufacturing workflow for a building component made with bamboo using AM technology. By leveraging AM's benefits and utilizing bamboo as a renewable and versatile material, this research seeks to promote sustainable practices in the field of architecture.

### *1.1. Agricultural Biowaste for Construction*

Over the last decade, the circular economy (CE) has gained significant attention for its potential to minimize environmental impacts and promote sustainability. The CE model focuses on maintaining resource value within the system, deviating from traditional management and playing a pivotal role in transforming biomass waste into raw materials. The use of agriculturally derived biowaste in construction is an emerging and sustainable practice that aligns with the principles of CE. Repurposing agricultural by-products and waste can reduce the negative environmental impacts of both the agriculture and construction industries.

The amount of biowaste generated by industrial sectors is rising in parallel with the increasing demand driven by the growing human population. Especially, food and agricultural industries generate enormous quantities of both liquid and solid waste in addition to that from various other contributing industries [4]. However, challenges, including the low competitiveness of bio-based products, hinder its full potential. Strategies like incorporating functionalized lignin in polymeric materials, biological and thermochemical treatments of bio-based waste, and producing bioplastics from agrifood waste have been explored in other research [5]. The incorporation of agriculturally derived biowastes in construction has the potential to not only provide a sustainable alternative to traditional materials but also help in managing agricultural residues effectively, contributing to a more circular and environmentally friendly construction industry. Even though several aspects related to the manufacturing process, energy use, and supply chain need further research, the use of biowaste in manufacturing applications shows potential for sustainability.

### *1.2. Additive Manufacturing with Agricultural Biowaste*

Integrating key enabling technologies (KETs) is essential for transitioning to a bioeconomy. Despite the challenges posed by the utilization of edible crops and concerns about low competitiveness, AM emerges as a pivotal technology in fostering CE models [6]. AM technology shows promise in recycling biodegradable polymers and fiber-reinforced polymers, underscoring their significance in the circular bioeconomy.

The international standard ISO/ASTM 52900:2001 defines AM as the general term for the process of joining materials to make parts from 3D model data, usually layer upon layer [7]. AM is distinct from conventional manufacturing techniques like subtractive procedures that generate a lot of waste material or formative processes that need molds to produce products in large quantities. Filling a need created by traditional manufacturing techniques, AM can advantageously fabricate complicated geometries with no part-specific tooling and significantly less waste material [8]. Based on the technique and materials, AM processes can be broadly divided into seven categories [9]:

- Vat photopolymerization (VP).
- Powder bed fusion (PBF) processes.
- Material extrusion (ME)-based systems.
- Material jetting (MJ).

- Binder jetting (BJ).
- Directed energy deposition (DED) processes.
- Sheet lamination (SL) processes.

In ME, the material is selectively dispensed through a nozzle or orifice [10]. In this research, fused deposition modeling (FDM), which is a type of ME, is explored. FDM is suggested as a method that offers greater design freedom, larger building volumes, and more cost-efficient production than liquid- and powder-based AM processes [11].

While AM processes have made substantial strides, there is a need for further research in the field of the built environment. This includes developing sustainable materials for construction, advancing the design methods and tools, and process optimization. The integration of innovative materials, such as geopolymer concrete and natural fiber-reinforced materials, has been explored [9]. However, the imperative remains to develop new materials capable of replacing materials that are not environmentally friendly. Therefore, the contemporary focus is on developing sustainable materials that are harmonious with advanced manufacturing techniques.

Rahman's systematic review of AM with a focus on agriculturally derived biowastes reveals that approximately 58% of the selected papers are from materials research [12]. The majority of biowastes originate from the agricultural, fishery, forestry, and agrifood industries. Notably, the development of novel materials for AM is still in its nascent stages, with polylactide (PLA) being the most commonly used material for biowaste-reinforced composites.

Romani's research systematically analyzes works related to biowaste for extrusion-based AM and identifies a notable increase in interest from 2019 to 2022 [6]. Environmental and social considerations were limited, despite the predominant focus on material science-related research. Most biowaste was derived from industrial and agricultural activities, emphasizing the paper, furniture, and timber industries. The utilization of polymers like PLA and its blends, ranging from 1% to 29% by weight, was prevalent.

In conclusion, the systematic reviews underscore the interest in leveraging AM for sustainable materials, mainly from agriculturally derived biowastes. Despite existing challenges, these reviews pave the way for future research, highlighting the imperative of holistic approaches that consider environmental, social, and economic sustainability. As industries increasingly embrace these materials, the transformative potential of AM in realizing a circular bioeconomy becomes more apparent, promising a paradigm shift towards a sustainable and resource-efficient future.

### *1.3. Additive Manufacturing with Bamboo*

Our literature review shows no commercial AM process utilizes bamboo as the sole feedstock. However, limited instances of AM involving bamboo fibers have been explored in other projects. These examples provide valuable insights into the state of the art concerning the utilization of bamboo in AM and offer essential information that informs the scope and objectives of the present research.

Gama's research chemically modified bamboo fibers via a two-step reaction, enhancing their compatibility with acrylonitrile butadiene styrene (ABS) in 3D printing [13]. The modified fibers demonstrated improved hydrophobicity, density, and thermal stability. Employing these treated fibers in 3D printing enhanced mechanical performance, as evidenced by improved melting flow index (MFI) and glass transition temperature (T<sub>g</sub>) values.

Soh introduced an extrudable paste using bamboo fiber, chitosan, and mycelium [14]. Optimal compositions with mycelium-enriched bamboo fibers and chitosan exhibited promising workability, extrudability, and buildability. Adding chitosan to mycelium-bound bamboo fibers resulted in a notable compression modulus increase, showcasing the potential for complex 3D forms.

Zhao investigated the bamboo powder-to-PLA ratio for 3D printing wire. The study identified an ecologically friendly bamboo powder–PLA composite with a 5:2 ratio, 2% plasticizer, and 2% lubricant [15]. This composite material exhibited smooth printing, wood-like texture, and consistent quality, meeting 3D-printing specifications.

Depuydt developed an FDM filament by compounding PLA with bamboo and flax fibers [16]. Comprehensive characterization, including fiber length-to-diameter ratios, revealed a substantial increase in the filament modulus (91% to 230%) with bamboo reinforcement. The study successfully printed a demonstrator part, illustrating the filament's practical application.

## 2. Materials and Experimental Research

### 2.1. Materials

#### 2.1.1. Binders

Commonly, binders refer to viscous liquids that can solidify through a chemical or physical reaction. Mixing them with filler materials (fibers or powder) binds the filler materials. Glue is one of the most commonly used binders. Four primary synthetic thermo-setting resins (phenol formaldehyde, urea formaldehyde, melamine–formaldehyde, and polymeric diphenylmethane diisocyanate resin) form the conventional base for wood composite adhesives. With an increasing interest in eco-friendly alternatives, renewable biomass resources like lignin, starch, plant proteins, tannin, bark, and vegetable oils are being explored. Kraft lignin can replace phenol due to its availability, processing ease, cost-effectiveness, and strong adhesion. Starch, known for its abundance, simplicity in processing, low cost, and adhesive capabilities, shows potential as a bio-adhesive feedstock. Plant proteins are also utilized to develop environmentally friendly wood adhesives [17].

Binders serve almost the same purpose as adhesives, creating a matrix to bind with fillers. This research identified the most frequently utilized bio-adhesives sourced from renewable materials, serving as a foundation for selecting appropriate binders for initial material trials. The selected binders were corn starch, potato starch, tapioca starch, gelatin, xanthan gum, collagen peptides, potato-based glue (an adhesive based on potato dextrins dissolved in water), and wood glue.

#### 2.1.2. Bamboo

Bamboo is a massive perennial grass belonging to the monocotyledon order of the angiosperms, the biggest member of the grass family [18]. Bamboo's rapid growth and productivity rate and quick harvest cycle make it a suitable building material, able to compensate for the high demand for wood [19].

Borowski's research suggests that planting an additional 10 million hectares of bamboo over 30 years could potentially offset the absorption of over 7 gigatons of CO<sub>2</sub> emissions, underscoring its substantial environmental contribution [2]. This positions bamboo as a promising material for climate change mitigation. Additionally, the same study highlights bamboo's rapid growth rate, with daily growth reaching up to 6 cm during its second and third weeks, accelerating to 37 cm in the following 4 days. By the third week, bamboo can achieve an impressive 80 cm of daily growth.

Bamboo presents a versatile alternative to conventional building materials, as demonstrated by various architectural projects such as the bamboo stalactite by VTN Architects and a house in Paranaque, Philippines, showcasing its use in trusses/roof structures, walls, flooring, scaffolding, and facades [20]. Habibi's review exemplifies approaches for using bamboo as a structural material in low-income housing through projects such as a prototype bamboo house designed by Ingvarsten Arkitekter, Blooming Bamboo home designed by H&P Architects, Pemulung House designed by BUKU, and Social Production of the Habitat designed by Comunal Taller de Arquitectura [21]. Also, Nurdiah's research explores bamboo as a suitable material for organically shaped

building construction through the Green School, OBI Great Hall, Dodoha Mosintuwu, and Bamboe Koening Restaurant projects [22]. However, this study diverges from typical applications by employing bamboo as powder and fibers.

In this research, specifically, three types of bamboo fibers and powder are utilized: bamboo fibers with length 1–3 mm and diameter 200–400  $\mu\text{m}$  (Figure 1a), brown bamboo powder with diameter 0–100  $\mu\text{m}$  (referred to as bamboo powder B for clarity) (Figure 1b), and green bamboo powder with diameter 0–100  $\mu\text{m}$ , sourced from *Sasa tsuboiana* stem and leaves (referred to as bamboo powder G for clarity) (Figure 1c). These powders are typically produced for agricultural applications to be used as soil fertilizer due to their organic composition. They can also be used to produce composite sheets through compression molding.



**Figure 1.** Bamboo material employed for research: (a) bamboo fibers; (b) bamboo powder B; (c) bamboo powder G.

## 2.2. Applied Research Design

Given the significance of design in generating new insights, knowledge, and practical–theoretical discourse that is accessible and endorsed by experts, this research adopts a research-by-design approach. The study capitalizes on existing digital design and fabrication technologies in architecture, particularly robotic AM, to explore the potential of bamboo as a renewable feedstock for bio-based construction materials. The research process is structured into four distinct phases: material exploration, printability exploration, geometry infill exploration, and concept design and prototyping. The experiments follow a material tinkering approach, which is defined as exploratory research to create a vision for a meaningful material experience to lead further development [23].

The material exploration phase involves exploring various material mixes, manually testing their viscosity and homogeneity, and assessing their printability (extrudability) using a manual extruder at room temperature. The results are documented for analysis and grading, which helps identify the most promising materials for subsequent mechanical testing.

The printability exploration phase extends the investigation into AM using an extruder mounted on a robot arm. Tests are designed to scrutinize parameters regarding the object properties, such as height, overhang, layer overlap, and infills, aiming to enhance our understanding of the advantages and limitations associated with creating a self-supporting wall.

The geometry infill exploration phase concentrates on probing the influence of potato starch on the geometry of printed objects, with a specific focus on improving material infill properties to improve structural performance. This is executed by printing diverse geometry infill patterns, which are subsequently subjected to compression testing.

The concept design and prototyping phase serves as a synthesis of knowledge acquired in earlier stages. It involves delineating a particular building component based on research findings. The chosen material compositions and printing processes are honed

during this phase to achieve optimal outcomes. The primary objective is to produce a partial prototype, validating the feasibility of AM with bamboo. The design process utilizes Rhino 7, a 3D modeling software package complemented by Grasshopper 1.0.007 (GH). GH is a visual programming interface and algorithmic design plug-in for Rhino. It is used to develop parametric designs and explore diverse design variations. In the context of this project, GH also contributes to determining the most efficient and effective design for the intended bamboo-based self-supporting wall and generating the program needed to fabricate it through robotic AM.

### 2.2.1. Manual Extrusion

The initial phase of material exploration was informed by the insights gained from the literature review. To formulate a bio-based recipe for extrusion, 27 experiments were conducted to investigate the performance of 8 different binders in combination with bamboo powder B and G, each with the addition of fiber. The preparation procedure varies according to the type of binder used. Binders such as corn starch, tapioca starch, gelatin, xanthan gum, and collagen peptides require water to transform into an adhesive. They are then combined with the fillers. On the other hand, binders like potato starch require water initially and then need to be boiled to form an adhesive before being mixed with the fillers. Additionally, potato-based glue and wood glue can be directly mixed with the powder to create a mixture. Therefore, the mixing and boiling procedure slightly varies based on the recipe. They all start with weighing the ingredients. The recipe with potato starch was prepared by combining the starch with water at room temperature until it was fully dissolved. Then, it was placed on an electric heating plate in a bowl. The mixture was continuously stirred until it reached boiling temperature, which took approximately 7 min. Then, a thick paste was formed and the mixture became transparent. It was then placed in a mixer, some dust added, and mixed. The remaining dust and fibers were added gradually, observing the mixture's viscosity towards extrusion based on prior experience.

This phase aimed to assess how the material mixture behaved with various binders and determine the most promising ones for further investigation in the extrusion printing phase. This exploration was carried out in two phases: the first focused on exploring the binding agents that could be used to develop an extrudable mixture, and it was regarded as a preliminary experiment. It was determined that a second phase was necessary to achieve a more comprehensive evaluation of the mix and to refine key parameters for more accurate and effective results in the extrusion printing phase.

The second phase of material exploration involved an evaluation method mainly based on the extrudability, mechanical strength, bio-based content, and cost of the material mixes. Ratios were determined through visual observations performed during the material mixing process. The observations focused primarily on geometrical deformations, such as the transformation of the form from its original state, changes in size and form due to shrinkage, and changes in surface texture. Other visual changes, such as color variation, were considered irrelevant to the objectives of this work; therefore, they were ignored. Binder-to-filler ratios are detailed in Table 1, and the material compositions can be found in Appendix A.

**Table 1.** The matrix of the second material exploration phase, presenting the binder-to-bamboo ratios.

	Bamboo Powder B	Bamboo Powder G	Bamboo Powder B + Bamboo Fibers	Bamboo Powder G + Bamboo Fibers
Corn starch	6:1	6:1	7.5:1	4.5:1
Potato starch	6:1	6:1	6:1	6:1
Tapioca starch	4:1	4:1	4:1	N/A
Gelatin	4:1	4:1	2.8:1	4:1

Xanthan gum	3:1	3:1	3:1	N/A
Collagen peptides	N/A	3.6:1	3.3:1	N/A
Potato-based glue	4:1	4:1	5:1	N/A
Wood glue	4:1	4:1	5:1	5:1

Mechanical strength testing in a laboratory setting was unfeasible due to the manual extrusion of the mixture, making traditional testing methods unreliable. Rather than conducting formal mechanical tests, an intuitive evaluation method was employed, assessing the specimen's performance with the following procedure. Each mixture's resistance to breakage and bending was evaluated by applying a 350 g weight at the center of each specimen. Specimens that failed under load were excluded from the next step of the research. Figure 2 delineates the various fillers utilized, comprising two types of powder (bamboo powder B and bamboo powder G), each supplemented with bamboo fibers (bamboo powder B + bamboo fibers and bamboo powder G + bamboo fibers). Conversely, the first column illustrates the array of binders employed: corn starch, potato starch, tapioca starch, gelatin, xanthan gum, collagen peptides, eco-friendly glue, and wood glue. The figure systematically illustrates the matrix combination of each filler with each binder.

Combination	Bamboo powder B	Bamboo powder G	Bamboo powder B + Bamboo fibers	Bamboo powder G + Bamboo fibers
Corn starch				
Potato starch				
Tapioca starch				n/a
Gelatin				
Xanthan Gum				n/a
Collagen Peptides	n/a			n/a
Ecologic glue				n/a
Wood glue				

**Figure 2.** Matrix of the second material exploration phase.

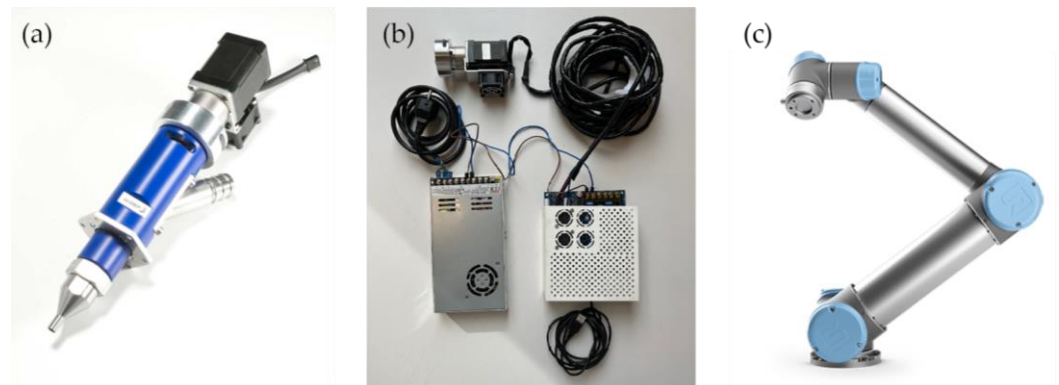
During the testing process, it was observed that glue is susceptible to drying faster in contact with air, making it difficult to extrude. However, potato starch was more convenient due to its ability to be reconstituted to its initial consistency by adding water, even if it dries during printing.

In conclusion, to proceed with the printing test, potato starch (marked in gray in Figure 2) is considered a promising binder due to its cost-effectiveness (compared with other binders tested), sustainability, and ease of use. These properties make it an affordable and readily available option for a wide range of users, with potential resistance being an added advantage.

### 2.2.2. Extrusion printing

Figure 3 shows the extrusion setup used for robotic AM. It includes the LDM WASP extruder XL 3.0 (Figure 3a), which regulates the extrusion amount. A stepper motor (Figure 3b) is attached to the motherboard and controls the extruder. The extruder and stepper motor are mounted on the UR5 six-axis robotic arm (Figure 3c).

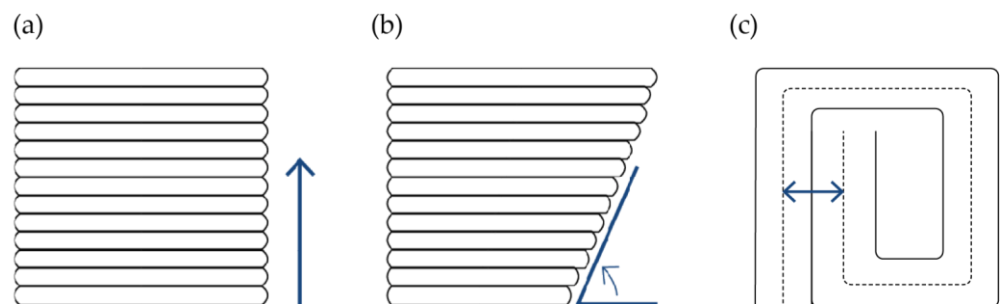




**Figure 3.** The extrusion setup used for robotic AM: (a) LDM WASP extruder XL 3.0 (image source: <https://www.3dwasp.shop> (accessed on 05.06.2023).); (b) stepper motor; (c) UR5 robotic arm (image source: <https://www.universal-robots.com> (accessed on 05.06.2023).).

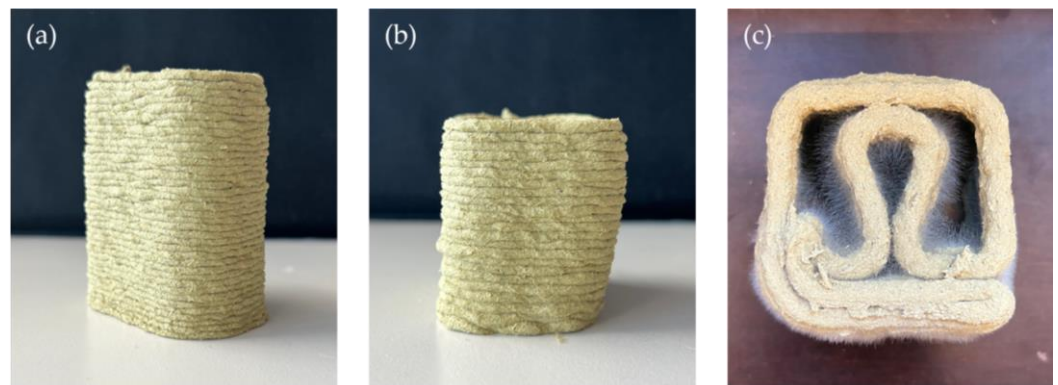
YAT 2.4.1 software was used to elaborate the G-code to operate the stepper motor. The G-code is necessary to ensure successful printing and calibrate the stepper motor's speed and pressure in accordance with the paste's consistency and nozzle diameter prior to incorporating robotic arm movements. This allows for the sending of commands to start and stop the stepper motor and specify its speed and number of spins.

The extrusion experiments explored the geometrical possibilities and limitations of designing a self-supporting wall. Specifically, three characteristics, shown in Figure 4, were explored: height, overhang, and infill overlap. The maximum printable height constrains the object's size that can be fabricated as a single piece (Figure 4a). Limitations regarding the overhangs inform about the possibilities related to the form concerning structural performance (Figure 4b). The infill overlap limits the minimum distance between two adjacent toolpath curves. In Figure 4c, the dashed line represents the toolpath followed by the center point of the extruder's nozzle, while the continuous lines represent the width of the extrusion. The objective is to identify the optimal distance at which adjacent tool paths would make contact to enable bounding while avoiding overlaps.



**Figure 4.** Testing parameters: (a) height; (b) overhang; (c) overlap.

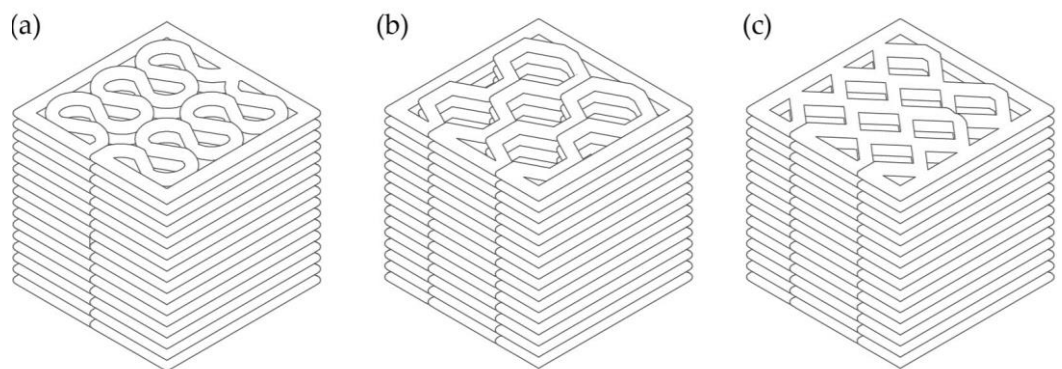
Each characteristic specimen was printed until it reached its limit: for height and overhang. The limits were determined by the point at which the specimen collapsed. The overlap was visually assessed until the walls no longer overlapped. Appendix B presents a comparison of height, overhang, and overlap explorations on printed specimens. Figure 5 shows the sample with the best performance achieved. It reached a height of 8 cm (Figure 5a) without collapsing on a rectangular footprint of 5 to 3 cm. It had an overhang up to 70 degrees relative to the printing base (Figure 5b). The minimum distance between the infill curves was set to 4 mm, which avoided overlaps along the infill with a 4 mm nozzle size (Figure 5c).



**Figure 5.** Printed specimen: (a) height of 8 cm; (b) overhang with a 70-degree slant; (c) overlap with a 4 mm gap.

### 2.2.3. Infill Design Exploration through Compression Testing

The design of the infill plays a crucial role in achieving the required structural performance, both during the printing process and in the design of the whole self-supporting wall. This research performed printing and mechanical tests to explore different infill geometries using the potato starch–bamboo mixture. This provides insight into the performance of both the material mix and the infill, and it sheds light on AM with bio-based materials in general. The research explores three infill designs, shown in Figure 6: curved (Figure 6a), honeycomb (Figure 6b), and rhombic (Figure 6c).



**Figure 6.** Infill geometries: (a) curved; (b) honeycomb; (c) rhombic.

A total of nine specimens were printed, three for each infill type with the same mixture composition. The specimens were dried in a dehydrator at 50 degrees Celsius for 24 h, weighed, and subjected to a compression test, as shown in Figure 7. It was observed that after 24 h, the specimens reached a visually stable state and did not continue changing. Therefore, this period was considered the optimal drying period. The color of the specimen changes during drying, and it exhibits a uniform color after it is completely dry. The tests were performed after the specimens were dry. However, the optimal drying time may vary depending on the size of the specimen.

The direction of testing is perpendicular to the layers. This corresponds to the expected design load on the designed component, detailed in Section 2.2.4. The tests provide force–displacement curves and the force and displacement at breakage. The experiment is not statistically representative enough to determine material properties. The goal was to investigate how different infill designs perform under a compression load. More specifically, the experiment compares the behavior of curved (Figure 7a), honeycomb (Figure 7b), and rhombic (Figure 7c) infill designs and assesses which has a higher resistance to compressive loading.



**Figure 7.** Compression test: (a) curved; (b) honeycomb; (c) rhombic.


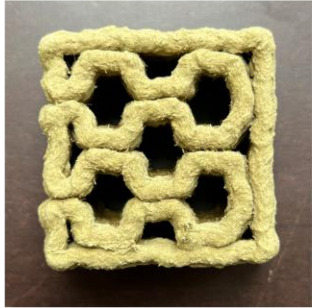
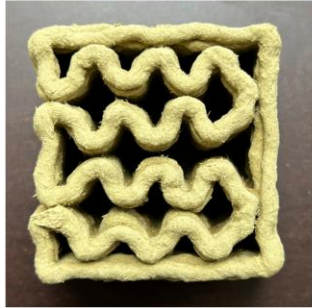



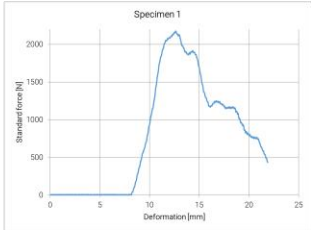
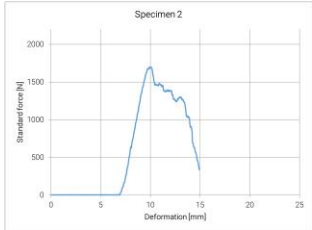
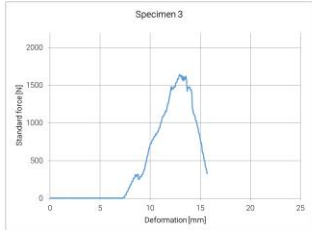
A Zwick Z100 electromechanical universal test machine (produced by ZwickRoell in Venlo, The Netherlands, available at the Mechanical Engineering Faculty of Delft University of Technology) was used for the compression tests. The results of the compression tests for all samples are presented in Appendix C. Figure 8 shows one result for each type of infill design, showing the piece before and after testing, the force–displacement curves, and the load at which the specimen broke. The primary objective of these tests was to observe how the specimens would break under compression load. Secondly, we aimed to observe if there was any clear correlation between fractures and numeric data, such as maximum load ( $F_{break}$ ) and maximum load per mass ( $F/m_{break}$ ) values. No such correlation was observed in these tests. However, the tests provided helpful insights into the fracture behaviors. It was observed that the corner represents the most vulnerable point of the specimens, and the more the layer overlapped on the side, the more resistant it was to breaking. The rhombic grid infill had the lowest performance among the three designs. The detachment of the sides from the vertices indicates that there may be insufficient bonding between the infill and the outer walls, which is a potential weakness that could affect the structure’s overall strength. It is also worth noting that while the rhombic grid infill did not break significantly in any of the samples, it did show signs of detachment and cracking, which could be a concern for applications requiring high strength and durability. Conversely, areas with less surface contact seem more prone to detachment, as was observed with the rhombic infill. Based on the results, the honeycomb infill design was identified as the best option for the objectives of this research.

The mechanical tests performed on the different infill patterns provide insights into their mechanical performance in two ways. The numeric results show the maximal load, and the breaking pattern shows the failure mode. The rhombic infill has a considerably lower performance on both accounts and is considered to have limited potential for this study. The curved infill performs best in terms of  $F_{break}$  and  $F/m_{break}$  values. It also has the highest material use and density. The breaking patterns show an overall failure of the specimen at the maximum load, resulting in extensive fragmentation. The honeycomb infill pattern has lower values, but it can be considered more efficient, considering its lower material use and less detachment after breaking. The double-wall structure improves the mechanical performance. The breaking pattern shows failure at the vertices of the patterns, which creates weak points due to their sharpness. Compared with the specimen with curved infill, the one with honeycomb infill shows less overall fragmentation.

The honeycomb infill pattern was selected for the next steps of this study, mainly due to the potential of the double-wall structure to improve (and also tailor) the mechanical performance. Rounding the printing path at the vertices can reduce the effect of the weak points, thus combining some of the strengths of the honeycomb and curved infill patterns.

The honeycomb structure has been extensively used in engineering applications and those requiring lightweight and high-mechanical-performance applications, such as the

aerospace, automotive, and construction industries, as well as interior design and furniture manufacturing [24–26].

	Curved	Honeycomb	Rhombic
Before test			
Weight	72 g	66.8 g	62.2 g
After test			
Graph			
F break	435 N	337 N	327 N
F/m break	6.04 N/g	5.04 N/g	5.26 N/g

**Figure 8.** Results of the compression test of the three specimens.

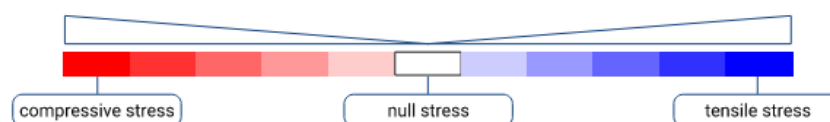
#### 2.2.4. Actual-Scale Prototyping

The research provides a proof of concept for AM of building components using bamboo composites by designing a self-supporting partition wall with an integrated bench and fabricating a partial mock-up of it on an actual scale. Figure 9 shows the wall's design concept, crafted by lofting through a sequence of freeform cross sections. These cross sections were specifically tailored to accommodate seating, providing adequate back support as they function as benches while maintaining a sufficient wall thickness to ensure self-support. The curves were designed to avoid sharp corners, which can cause problems during fabrication, such as excessive extrusion, due to the circular nozzle and the fact that it followed the extrusion toolpath with a constant speed without changing its orientation. Also, the initial experiments had shown that smooth curves allow higher printing performance than sharp corners. The curves extend on both sides of the wall to allow seating surfaces to be integrated into the wall.



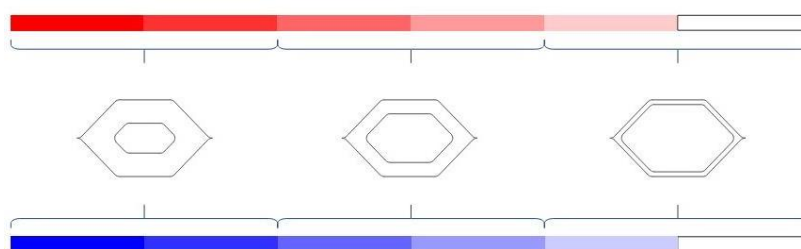
**Figure 9.** The design concept of the self-supporting wall.

AM allows for intricate performance-based designs. Within the context of this research, the prominent feature of AM was the efficient use of materials by precisely depositing material only where it is needed. Using the visual programming language GH, the developed algorithm and parametric definition capitalize on this feature by optimizing the material distribution based on the loads imposed on the designed structure. The parametric definition developed in GH was used to generate a mechanically informed infill design within specified spatial constraints, accounting for loads and boundary conditions through an iterative process. It varies the density of the infill based on the type and magnitude of the internal stresses. The algorithm integrates a structural analysis using Karamba3D 2.2.0, a GH plug-in for finite element analysis. The analysis provides the utilization factor, which shows the ratio between the stress and the material capacity in a given area. A lower utilization factor means the material is underutilized and could be reduced in the respective location. The algorithm represents the utilization through a color gradient, shown in Figure 10: red and blue represent the limits for compressive and tensile stress, respectively, while white represents a neutral or null stress state. The transitional gradients between these extreme colors form the intermediate shades.



**Figure 10.** Color gradient for utilization.

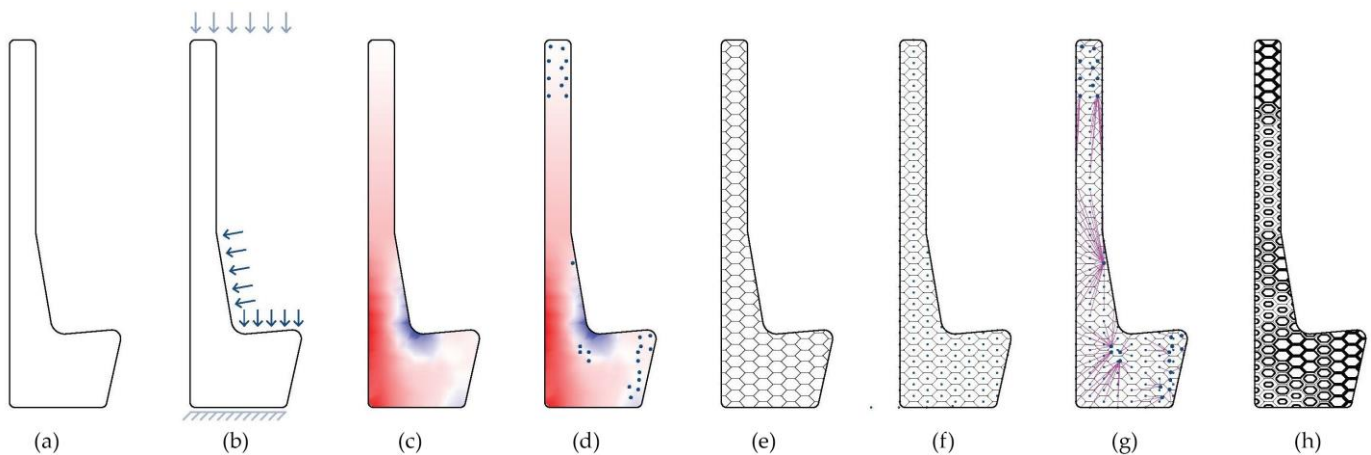
To achieve a mechanically informed infill design, the algorithm applies a consistent pattern with uniform cell size over the entire component while allowing for variable cell wall thickness. As a result, increasing utilization leads to thicker wall thickness, as shown in Figure 11. This approach ensures that the infill design is optimized for varying stress conditions throughout the component based on the varying utilization. This enhances the overall material efficiency of the component.



**Figure 11.** Infill design optimization through customized wall thickness concerning stress conditions.

Figure 12 shows the main steps of the design process through a cross section of the wall. The first step is the generation of the mesh geometry of the design (Figure 12a). This mesh is then imported into Karamba3D, where the type of support and load conditions are calculated (Figure 12b; the arrows show the directions of the considered loads). This calculation's output is represented through a color gradient that represents the stress distribution within the wall (Figure 12c). Within this color gradient, the parts with the lowest stress are identified as attractor points (Figure 12d). These attractor points are reference points for generating the infill pattern in the next step.

The generation of the honeycomb pattern (Figure 12e) is accomplished using the Ngon 2.1 plug-in, which automatically creates a pattern within the geometry boundary. The center point of each honeycomb cell is highlighted (Figure 12f). Each center point is connected to the closest attractor point, and the distances between them are divided into three segments (Figure 12g). These segments correspond to the three different thicknesses to be employed in the infill design. The thickness assigned to each section is inversely proportional to the distance, meaning that shorter distances result in greater thinness. Through this method, the infill pattern is created, taking into account the stress distribution within the component (Figure 12h). This approach ensures that the infill is optimized for the specific loads on the component, resulting in more efficient use of materials and better overall structural performance. The chosen design represents just one of the possibilities that can be implemented. Alternative designs can be developed to meet specific requirements and constraints depending on the specific space and function where the component will be placed.



**Figure 12.** Mechanically informed infill design process: (a) geometry mesh generation; (b) definition of loads and supports; (c) utilization output; (d) attractor points; (e) infill geometry; (f) centroid; (g) distance from the center point to attractor point; (h) generated informed infill.

The simulation was conducted for a two-dimensional segment of the design, considering the loads that apply to this specific cross section. It is presumed that the whole self-supporting wall would be divided into segments for fabrication. Then, the cross section of each segment would be simulated to develop the infill design specific to that segment. The segmentation of the whole self-supporting wall for fabrication is suggested due to the limitations of the robotic arm's reach and the maximum printable height.

To demonstrate this concept design through a tangible prototype, part of it was fabricated on an actual scale (Figure 13). The prototype's dimension was limited to the robotic arm's maximum reach. The prototype shows the changing void size of the hexagonal infill cells concerning the calculated load conditions on the component. While the fabricated prototype represents a small portion of the overall design, it serves as a tangible proof of concept and provides valuable insights into the feasibility and potential of printing with bamboo.



Figure 13. Prototyping.

### 3. Discussion

This proof of concept of AM with a novel bamboo–potato starch mixture shows potential for further development and optimization.

The experiments show that the mechanical properties of the printed material are still limited. Material research presents numerous opportunities to improve it. A thorough analysis of different types of bamboo powder and fibers can provide more detailed insights into the mechanical behavior of different material compositions. Further studies on bio-based binders can help identify alternatives to potato starch that can enhance the mechanical performance of the composite material. Additionally, investigating mold growth during the drying process, influenced by the water content, can lead to the development of preventive measures and a better understanding of its impact on the material structure and properties. Refining the proportion of materials used and optimizing the mixing process are crucial areas for future investigation. Exploring the maximum quantity of fibers that can be implemented without causing the nozzle to clog is essential to achieving more desirable mechanical properties. The effect of fiber orientation on the material's behavior should also be thoroughly examined.

This study included compression tests of small-scale components. The results provide insight into the failure mechanisms and the relationship between the design of the component infill and its mechanical performance. More tests are required to generalize these results. Based on the outcomes of this study, future research could investigate optimization routines, e.g., topology optimization, to further tailor and improve the performance of the infill designs. Tensile and bending strength testing may provide valuable insights into the properties of the components made of bamboo and potato starch to create spanning structures or cantilevers.

While strength testing on small specimens provides initial data, it may not directly translate to larger structures. Future research should compare the results from small specimens to those of full-scale structures to more accurately understand the influence of size on mechanical properties.

Concerning AM, more extensive research should be conducted on the impact of geometry. Investigating and overcoming the limitations encountered during the fabrication process, such as overhangs, will unlock new possibilities for complex geometries.

Additionally, exploring the integration of AM with other fabrication methods can lead to innovative and more effective approaches in construction.

On the design front, countless possibilities exist for further exploration. Interior applications can involve creating different objects to showcase the material's versatility. For exterior applications, rigorous investigations are needed to ensure the building components can withstand external weather conditions.

The drying phase required diligent attention. As a fully bio-based material, the wet prototype attracted fruit flies, which must be addressed promptly. The prototype had to be carefully brushed using vinegar to prevent mold growth. Shrinkage became a significant issue during the full-scale prototype's drying process. Figure 14 shows the prototype before and after drying.



**Figure 14.** Printed prototype before (left) and after (right) drying.

The shape of the prototype underwent substantial changes, resulting in cracks. This can have a negative impact on the overall mechanical performance of the component. This aspect underscores the need for further research to understand the underlying factors contributing to shrinkage and to explore potential mitigation methods. Future investigations can focus on optimizing the drying process parameters, such as temperature and humidity, as well as exploring alternative materials or additives to minimize shrinkage and enhance the structural integrity of the prototypes.

The full-scale prototype showed some limitations concerning the scaling of the process and method. The height of the prototype was limited by time constraints. However, based on the stability observed during the printing process, it is reasonable to assume that a greater height could be achieved with the material mixture. One approach to overcome height limitations is to divide the component into smaller sections that can be assembled after printing. These parts could be connected using the material mixture as a form of adhesive, allowing them to dry and bond together. Alternatively, an interlocking assembly design could be explored to avoid the need for adhesive and facilitate dry assembly. The size (length and width) of the component is restricted by the robotic arm's reach. To manufacture larger pieces, smaller components may need to be assembled after fabrication. In this case, the design of the joints between different pieces becomes crucial.



Recycling of fabricated components can be achieved by breaking them into small pieces, adding water to return them to a liquid form, and incorporating them into new mixtures for re-fabrication. This process allows for a sustainable cycle of material use.

Consideration of additives to improve performance, whether for structural reinforcement or other purposes such as waterproofing or fireproofing, is essential. Additives can enhance the material's properties to withstand heavier loads or external environmental factors, expanding its potential applications.

**Author Contributions:** Conceptualization, J.W., S.A. and S.B.; methodology, J.W.; software, J.W.; validation, J.W.; formal analysis, J.W.; investigation, J.W.; resources, J.W.; data curation, J.W.; writing—original draft preparation, J.W.; writing—review and editing, S.A. and S.B.; visualization, J.W.; supervision, S.A. and S.B. All authors have read and agreed to the published version of the manuscript.

**Funding:** This research received no external funding.

**Institutional Review Board Statement:** Not applicable.

**Informed Consent Statement:** Not applicable.

**Data Availability Statement:** The original contributions presented in the study are included in the article. Further inquiries can be directed to the corresponding authors.

**Acknowledgments:** This article was developed based on the master's graduation thesis of J. Wong [27], which was supervised by S. Aşut (first mentor) and S. Brancart (second mentor). This research was made possible thanks to the contributions of Bambooder and Made In Bamboo, who donated the bamboo dust and fibers.

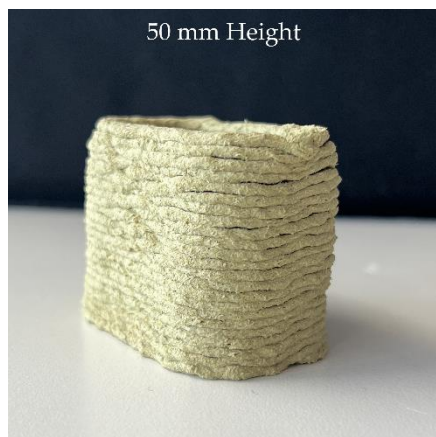
**Conflicts of Interest:** The authors declare no conflicts of interest.

#### Appendix A. The material compositions

Binder	Bamboo Powder B	Bamboo Powder G	Bamboo Powder B + Bamboo Fibers	Bamboo Powder G + Bamboo Fibers
Corn starch	Corn starch: 10 g Water: 50 g Bamboo powder: 10 g	Corn starch: 10 g Water: 50 g Bamboo powder: 10 g	Corn starch: 10 g Water: 50 g Bamboo powder: 3 g Bamboo fibers: 5 g	Corn starch: 10 g Water: 50 g Bamboo powder: 10 g Bamboo fibers: 3 g
Potato starch	Potato starch: 5 g Water: 25 g Bamboo powder: 5 g	Potato starch: 5 g Water: 25 g Bamboo powder: 5 g	Potato starch: 5 g Water: 25 g Bamboo powder: 3 g Bamboo fibers: 2 g	Potato starch: 5 g Water: 25 g Bamboo powder: 2 g Bamboo fibers: 3 g
Tapioca starch	Tapioca starch: 10 g Water: 10 g Bamboo powder: 5 g	Tapioca starch: 10 g Water: 10 g Bamboo powder: 5 g	Tapioca starch: 10 g Water: 10 g Bamboo powder: 3 g Bamboo fibers: 2 g	n/a
Gelatin	Gelatin sheet: 2 g Water: 20 g Bamboo powder: 5 g	Gelatin sheet: 2 g Water: 20 g Bamboo powder: 5 g	Gelatin sheet: 2 g Water: 20 g Bamboo powder: 5 g Bamboo fibers: 2 g	Gelatin sheet: 2 g Water: 20 g Bamboo powder: 5 g Bamboo fibers: 2 g
Xanthan gum	Xanthan gum: 10 g Water: 15 g Bamboo powder: 5 g	Xanthan gum: 10 g Water: 15 g Bamboo powder: 5 g	Xanthan gum: 10 g Water: 15 g Bamboo powder: 3 g Bamboo fibers: 2 g	n/a
Collagen peptides	n/a	Collagen peptides: 8 g Water: 10 g Bamboo powder: 5 g	Collagen peptides: 6 g Water: 4 g Bamboo powder: 2 g Bamboo fibers: 1 g	n/a
Potato-based glue	Potato-based glue: 20 g Bamboo powder: 5 g	Potato-based glue: 20 g Bamboo powder: 5 g	Potato-based glue: 20 g Bamboo powder: 2 g Bamboo fibers: 2 g	n/a
Wood glue	Wood glue: 20 g Bamboo powder: 5 g	Wood glue: 20 g Bamboo powder: 5 g	Wood glue: 20 g Bamboo powder: 2 g Bamboo fibers: 2 g	Wood glue: 20 g Bamboo powder: 2 g Bamboo fibers: 2 g

**Appendix B.** Height, overhang, and overlap comparisons between the printed specimens

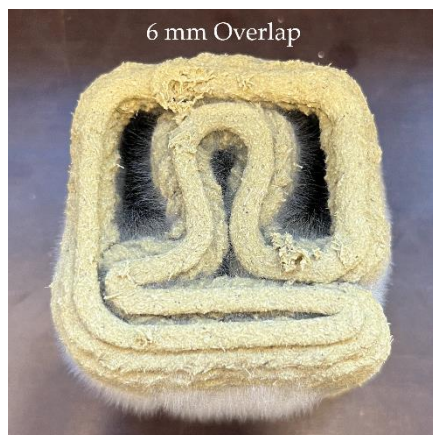
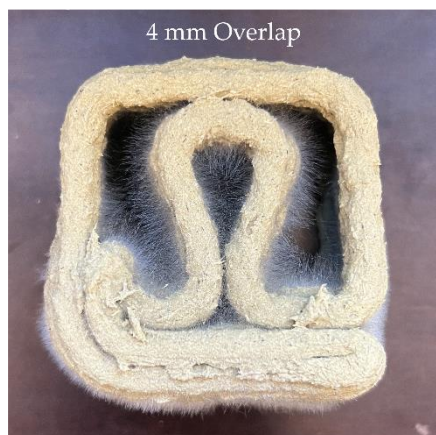
**Height Comparison**




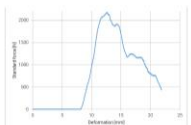


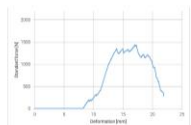


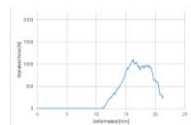


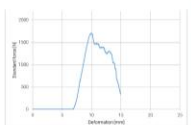


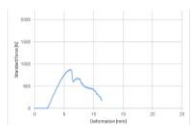


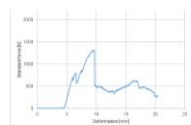


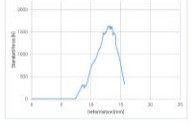


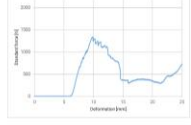


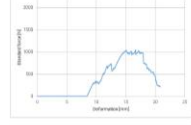

**Overhang Comparison**



**Overlap Comparison**



## Appendix C. Compression test results

Mixture Geometry	Bamboo powder G + Fibers	Bamboo powder B + Fibers	Bamboo powder B + Fibers																														
Curved	<table border="1"> <tr><td>Weight</td><td>72 g</td></tr> <tr><td>F max</td><td>2177 N</td></tr> <tr><td>dL at F max</td><td>12.6 mm</td></tr> <tr><td>F break</td><td>435 N</td></tr> <tr><td>dL at F break</td><td>21.8 mm</td></tr> </table>   	Weight	72 g	F max	2177 N	dL at F max	12.6 mm	F break	435 N	dL at F break	21.8 mm	<table border="1"> <tr><td>Weight</td><td>43.6 g</td></tr> <tr><td>F max</td><td>1443 N</td></tr> <tr><td>dL at F max</td><td>16.9 mm</td></tr> <tr><td>F break</td><td>283 N</td></tr> <tr><td>dL at F break</td><td>21.8 mm</td></tr> </table>   	Weight	43.6 g	F max	1443 N	dL at F max	16.9 mm	F break	283 N	dL at F break	21.8 mm	<table border="1"> <tr><td>Weight</td><td>34.9 g</td></tr> <tr><td>F max</td><td>1099 N</td></tr> <tr><td>dL at F max</td><td>16.3 mm</td></tr> <tr><td>F break</td><td>219 N</td></tr> <tr><td>dL at F break</td><td>21.3 mm</td></tr> </table>   	Weight	34.9 g	F max	1099 N	dL at F max	16.3 mm	F break	219 N	dL at F break	21.3 mm
Weight	72 g																																
F max	2177 N																																
dL at F max	12.6 mm																																
F break	435 N																																
dL at F break	21.8 mm																																
Weight	43.6 g																																
F max	1443 N																																
dL at F max	16.9 mm																																
F break	283 N																																
dL at F break	21.8 mm																																
Weight	34.9 g																																
F max	1099 N																																
dL at F max	16.3 mm																																
F break	219 N																																
dL at F break	21.3 mm																																
Honeycomb	<table border="1"> <tr><td>Weight</td><td>66.8 g</td></tr> <tr><td>F max</td><td>1702 N</td></tr> <tr><td>dL at F max</td><td>10 mm</td></tr> <tr><td>F break</td><td>337 N</td></tr> <tr><td>dL at F break</td><td>14.9 mm</td></tr> </table>   	Weight	66.8 g	F max	1702 N	dL at F max	10 mm	F break	337 N	dL at F break	14.9 mm	<table border="1"> <tr><td>Weight</td><td>68.5 g</td></tr> <tr><td>F max</td><td>879 N</td></tr> <tr><td>dL at F max</td><td>6.13 mm</td></tr> <tr><td>F break</td><td>175.5 N</td></tr> <tr><td>dL at F break</td><td>11.4 mm</td></tr> </table>   	Weight	68.5 g	F max	879 N	dL at F max	6.13 mm	F break	175.5 N	dL at F break	11.4 mm	<table border="1"> <tr><td>Weight</td><td>45.7 g</td></tr> <tr><td>F max</td><td>1308 N</td></tr> <tr><td>dL at F max</td><td>9.6 mm</td></tr> <tr><td>F break</td><td>261.7 N</td></tr> <tr><td>dL at F break</td><td>20.4 mm</td></tr> </table>   	Weight	45.7 g	F max	1308 N	dL at F max	9.6 mm	F break	261.7 N	dL at F break	20.4 mm
Weight	66.8 g																																
F max	1702 N																																
dL at F max	10 mm																																
F break	337 N																																
dL at F break	14.9 mm																																
Weight	68.5 g																																
F max	879 N																																
dL at F max	6.13 mm																																
F break	175.5 N																																
dL at F break	11.4 mm																																
Weight	45.7 g																																
F max	1308 N																																
dL at F max	9.6 mm																																
F break	261.7 N																																
dL at F break	20.4 mm																																
Rhombic	<table border="1"> <tr><td>Weight</td><td>62.2 g</td></tr> <tr><td>F max</td><td>1641 N</td></tr> <tr><td>dL at F max</td><td>12.9 mm</td></tr> <tr><td>F break</td><td>327 N</td></tr> <tr><td>dL at F break</td><td>15.6 mm</td></tr> </table>   	Weight	62.2 g	F max	1641 N	dL at F max	12.9 mm	F break	327 N	dL at F break	15.6 mm	<table border="1"> <tr><td>Weight</td><td>53.6 g</td></tr> <tr><td>F max</td><td>1339 N</td></tr> <tr><td>dL at F max</td><td>9.87 mm</td></tr> <tr><td>F break</td><td>265 N</td></tr> <tr><td>dL at F break</td><td>28.8 mm</td></tr> </table>   	Weight	53.6 g	F max	1339 N	dL at F max	9.87 mm	F break	265 N	dL at F break	28.8 mm	<table border="1"> <tr><td>Weight</td><td>40.1 g</td></tr> <tr><td>F max</td><td>1043 N</td></tr> <tr><td>dL at F max</td><td>15.1 mm</td></tr> <tr><td>F break</td><td>208 N</td></tr> <tr><td>dL at F break</td><td>20.8 mm</td></tr> </table>   	Weight	40.1 g	F max	1043 N	dL at F max	15.1 mm	F break	208 N	dL at F break	20.8 mm
Weight	62.2 g																																
F max	1641 N																																
dL at F max	12.9 mm																																
F break	327 N																																
dL at F break	15.6 mm																																
Weight	53.6 g																																
F max	1339 N																																
dL at F max	9.87 mm																																
F break	265 N																																
dL at F break	28.8 mm																																
Weight	40.1 g																																
F max	1043 N																																
dL at F max	15.1 mm																																
F break	208 N																																
dL at F break	20.8 mm																																

## References

- Craveiro, F.; Duarte, J.P.; Bartolo, H.; Bartolo, P.J. Additive manufacturing as an enabling technology for digital construction: A perspective on Construction 4.0. *Autom. Constr.* **2019**, *103*, 251–267. <https://doi.org/10.1016/j.autcon.2019.03.011>.
- Borowski, P.F.; Patuk, I.; Bandala, E.R. Innovative Industrial Use of Bamboo as Key “Green” Material. *Sustainability* **2022**, *14*, 1955. <https://doi.org/10.3390/su14041955>.
- Stegmann, P.; Londo, M.; Junginger, M. The circular bioeconomy: Its elements and role in European bioeconomy clusters. *Resour. Conserv. Recycl. X* **2020**, *6*, 100029. <https://doi.org/10.1016/j.rcrx.2019.100029>.
- Ravindran, B.; Karmegam, N.; Yuvaraj, A.; Thangaraj, R.; Chang, S.W.; Zhang, Z.; Kumar Awasthi, M. Cleaner production of agriculturally valuable benignant materials from industry generated bio-wastes: A review. *Bioresour. Technol.* **2021**, *320*, 124281. <https://doi.org/10.1016/j.biortech.2020.124281>.
- Usmani, Z.; Sharma, M.; Karpichev, Y.; Pandey, A.; Chander Kuhad, R.; Bhat, R.; Punia, R.; Aghbashlo, M.; Tabatabaei, M.; Gupta, V.K. Advancement in valorization technologies to improve utilization of bio-based waste in bioeconomy context. *Renew. Sustain. Energy Rev.* **2020**, *131*, 109965. <https://doi.org/10.1016/j.rser.2020.109965>.
- Romani, A.; Suriano, R.; Levi, M. Biomass waste materials through extrusion-based additive manufacturing: A systematic literature review. *J. Clean. Prod.* **2023**, *386*, 135779. <https://doi.org/10.1016/j.jclepro.2022.135779>.
- ISO/ASTM 52900:2021; Additive Manufacturing—General Principles—Fundamentals and Vocabulary. ASTM International: West Conshohocken, PA, USA, 2021.
- Delgado Camacho, D.; Clayton, P.; O'Brien, W.J.; Seepersad, C.; Juenger, M.; Ferron, R.; Salamone, S. Applications of additive manufacturing in the construction industry—A forward-looking review. *Autom. Constr.* **2018**, *89*, 110–119. <https://doi.org/10.1016/j.autcon.2017.12.031>.
- Al Rashid, A.; Khan, S.A.; Al-Ghamdi, S.G.; Koç, M. Additive manufacturing: Technology, applications, markets, and opportunities for the built environment. *Autom. Constr.* **2020**, *118*, 103268. <https://doi.org/10.1016/j.autcon.2020.103268>.
- Romani, A.; Rognoli, V.; Levi, M. Design, Materials, and Extrusion-Based Additive Manufacturing in Circular Economy Contexts: From Waste to New Products. *Sustainability* **2021**, *13*, 7269. <https://doi.org/10.3390/su13137269>.
- Altıparmak, S.C.; Yardley, V.A.; Shi, Z.; Lin, J. Extrusion-based additive manufacturing technologies: State of the art and future perspectives. *J. Manuf. Process.* **2022**, *83*, 607–636. <https://doi.org/10.1016/j.jmapro.2022.09.032>.

12. Rahman, A.M.; Rahman, T.T.; Pei, Z.; Ufodike, C.O.; Lee, J.; Elwany, A. Additive Manufacturing Using Agriculturally Derived Biowastes: A Systematic Literature Review. *Bioengineering* **2023**, *10*, 845. <https://doi.org/10.3390/bioengineering10070845>.
13. Gama, N.; Magina, S.; Ferreira, A.; Barros-Timmons, A. Chemically modified bamboo fiber/ABS composites for high-quality additive manufacturing. *Polym. J.* **2021**, *53*, 1459–1467. <https://doi.org/10.1038/s41428-021-00540-9>.
14. Soh, E.; Chew, Z.Y.; Saeidi, N.; Javadian, A.; Hebel, D.; Le Ferrand, H. Development of an extrudable paste to build mycelium-bound composites. *Mater. Des.* **2020**, *195*, 109058. <https://doi.org/10.1016/j.matdes.2020.109058>.
15. Zhao, D.X.; Cai, X.; Shou, G.Z.; Gu, Y.Q.; Wang, P.X. Study on the Preparation of Bamboo Plastic Composite Intend for Additive Manufacturing. *Key Eng. Mater.* **2015**, *667*, 250–258. <https://doi.org/10.4028/www.scientific.net/KEM.667.250>.
16. Depuydt, D.; Balthazar, M.; Hendrickx, K.; Six, W.; Ferraris, E.; Desplentere, F.; Ivens, J.; Van Vuure, A.W. Production and characterization of bamboo and flax fiber reinforced polylactic acid filaments for fused deposition modeling (FDM). *Polym. Compos.* **2019**, *40*, 1951–1963. <https://doi.org/10.1002/pc.24971>.
17. Ferdosian, F.; Pan, Z.; Gao, G.; Zhao, B. Bio-Based Adhesives and Evaluation for Wood Composites Application. *Polymer* **2017**, *9*, 70. <https://doi.org/10.3390/polym9020070>.
18. Goh, Y.; Yap, S.P.; Tong, T.Y. Bamboo: The Emerging Renewable Material for Sustainable Construction. In *Encyclopedia of Renewable and Sustainable Materials*; Elsevier: Amsterdam, The Netherlands, 2020; pp. 365–376.
19. Richard, M.J. Assessing the Performance of Bamboo Structural Components. Doctoral Dissertation, University of Pittsburgh, Pittsburgh, PA, USA, 2013.
20. Yadav, M.; Mathur, A. Bamboo as a sustainable material in the construction industry: An overview. *Mater. Today Proc.* **2021**, *43*, 2872–2876. <https://doi.org/10.1016/j.matpr.2021.01.125>.
21. Habibi, S. Design concepts for the integration of bamboo in contemporary vernacular architecture. *Archit. Eng. Des. Manag.* **2019**, *15*, 475–489. <https://doi.org/10.1080/17452007.2019.1656596>.
22. Nurdiah, E.A. The Potential of Bamboo as Building Material in Organic Shaped Buildings. *Procedia Soc. Behav. Sci.* **2016**, *216*, 30–38. <https://doi.org/10.1016/j.sbspro.2015.12.004>.
23. Parisi, S.; Rognoli, V.; Sonneveld, M. Material Tinkering. An inspirational approach for experiential learning and envisioning in product design education. *Des. J.* **2017**, *20*, S1167–S1184. <https://doi.org/10.1080/14606925.2017.1353059>.
24. Ayrlimis, N.; Kariz, M.; Šernek, M.; Kuzman, M.K. Effects of sandwich core structure and infill rate on mechanical properties of 3D-printed wood/PLA composites. *Int. J. Adv. Manuf. Technol.* **2021**, *115*, 3233–3242. <https://doi.org/10.1007/s00170-021-07382-y>.
25. Habib, F.N.; Iovenitti, P.; Masood, S.H.; Nikzad, M. Cell geometry effect on in-plane energy absorption of periodic honeycomb structures. *Int. J. Adv. Manuf. Technol.* **2017**, *94*, 2369–2380. <https://doi.org/10.1007/s00170-017-1037-z>.
26. Araújo, H.; Leite, M.; Ribeiro, A.R.; Deus, A.M.; Reis, L.; Vaz, M.F. The effect of geometry on the flexural properties of cellular core structures. *Proc. Inst. Mech. Eng. Part L J. Mater. Des. Appl.* **2019**, *233*, 338–347. <https://doi.org/10.1177/1464420718805511>.
27. Wong, J. Breaking Ground with Bamboo: Robotic Additive Manufacturing of a Self Supporting Wall with Bamboo. Master's Thesis, Delft University of Technology, Delft, The Netherlands, 2023.

**Disclaimer/Publisher's Note:** The statements, opinions and data contained in all publications are solely those of the individual author(s) and contributor(s) and not of MDPI and/or the editor(s). MDPI and/or the editor(s) disclaim responsibility for any injury to people or property resulting from any ideas, methods, instructions or products referred to in the content.